



Open Research Online

Citation

White, Glenn J.; Doi, Yasuo; Komugi, Shinya; Kawada, Mitsunobu; Takita, Satoshi; Arimatsu, Ko; Ikeda, Norio; Kato, Daisuke; Kitamura, Yoshimi; Nakagawa, Takao; Ootsubo, Takafumi; Morishima, Takahiro; Hattori, Makoto; Tanaka, Masahiro; Etxaluze, Mireya and Shibai, Hiroshi (2012). The filamentary web of star formation. Publications of The Korean Astronomical Society, 27(4) pp. 201–207.

URL

<https://oro.open.ac.uk/36487/>

License

(CC-BY-NC-ND 4.0)Creative Commons: Attribution-Noncommercial-No Derivative Works 4.0

Policy

This document has been downloaded from Open Research Online, The Open University's repository of research publications. This version is being made available in accordance with Open Research Online policies available from [Open Research Online \(ORO\) Policies](#)

Versions

If this document is identified as the Author Accepted Manuscript it is the version after peer review but before type setting, copy editing or publisher branding

THE FILAMENTARY WEB OF STAR FORMATION

GLENN J. WHITE^{1,2}, YASUO DOI³, SHINYA KOMUGI^{4,5}, MITSUNOBU KAWADA⁵, SATOSHI TAKITA⁵, KO ARIMATSU⁵, NORIO IKEDA⁵, DAISUKE KATO⁵, YOSHIMI KITAMURA⁵, TAKAO NAKAGAWA⁵, TAKAFUMI OOTSUBO⁶, TAKAHIRO MORISHIMA⁶, MAKOTO HATTORI⁶, MASAHIRO TANAKA⁷, MIREYA ETXALUZE^{1,2,8}, AND HIROSHI SHIBAI⁹

¹Department of Physical Sciences, The Open University, England

²RALSpace, The Rutherford Appleton Laboratory, Chilton, Didcot, Oxfordshire OX11 0NL, England

³Department of Earth Science and Astronomy, the University of Tokyo, Tokyo 153-8902, Japan

⁴Joint ALMA Observatory, Alonso de Cordova 3107, Vitacura, Santiago 763-0355, Chile

⁵Institute of Space and Astronautical Science, Japan Aerospace Exploration Agency, Kanagawa 252-5210, Japan

⁶Astronomical Institute, Tohoku University, Sendai 980-8578, Japan

⁷Center for Computational Sciences, University of Tsukuba, Ibaraki 305-8577, Japan

⁸Centro de Astrobiología (CSIC/INTA), Instituto Nacional de Técnica Aeroespacial, Madrid Spain

⁹Department of Earth and Space Science, Osaka University, Osaka 560-0043, Japan

E-mail: g.j.white@open.ac.uk

(Received July 08, 2012; Accepted July 25, 2012)

ABSTRACT

Following the first Public Release of the AKARI Point Source catalogues, we have worked on the production of a new far-infrared All-Sky Diffuse mapping product. In this paper we report first results from the All Sky diffuse maps that will shortly be released to the community, based on analysis of data from the Far Infrared Surveyor (65 μm - 160 μm) instrument. These data are likely to have a strong impact on studies of extended structures, and the diffuse ISM.

Key words: infrared: telescope; conferences: proceedings

1. INTRODUCTION

A major issue in contemporary star formation research is to improve our understanding of the mechanisms involved in the formation of stars, and their attendant planetary systems. We provide an update on the status of the AKARI All Sky Diffuse Mapping project, and present some early results from large-scale images, focussing on the study and characterisation of the Filamentary Web linking star-formation throughout our Galaxy, and revealing its association with pre-stellar cores and protostars. We report the first stages of a study that seeks to establish a link between the pre-stellar core mass function and the stellar IMF; to trace and map the formation of stars and clusters along the initially quiescent filaments that thread the ISM; and to determine whether the IMF is determined at the

pre-stellar core formation stage.

The associated diffuse infrared continuum emission is ubiquitously observed across the sky, and is attributed to thermal emission from interstellar dust particles. These dust particles are heated by incident stellar radiation in the UV, optical and near-infrared spectral regions, with a peak at around 1 μm (the interstellar radiation field: ISRF; Mathis et al., 1983), and then re-radiating the thermal energy at longer wavelengths in the far-infrared and sub-mm wavelength regions.

2. AKARI FAR-INFRARED DIFFUSE ALL SKY SURVEY

The AKARI space telescope, launched by ISAS/JAXA in 2006 (Murakami et al., 2007), successfully carried out an all sky survey in six bands at mid- and far-infrared

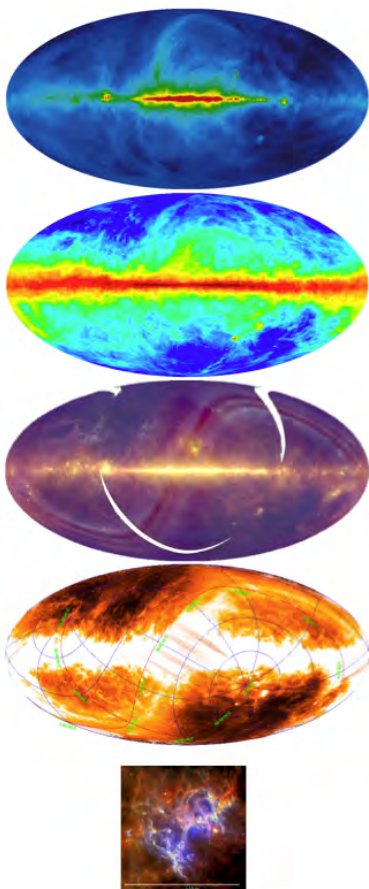


Fig. 1. All sky images, from top to bottom: 408 MHz radio continuum: 21 cm atomic hydrogen line: IRAS 60 μm : AKARI 90 μm all sky diffuse map: Herschel observations of the Eagle Nebula from Hill et al. (2012).

wavelengths, as well as obtaining pointed observations for several large area surveys of the near and far Universe, as well as obtaining many deep pointed observations on specific targets. The satellite was launched in February 2006 and the all-sky survey was carried out between March 2006–August 2007 during the cold operational phase before the liquid Helium cryogen was exhausted. AKARI’s mirror had a diameter of 0.685 m and was capable to observe across the 2–180 μm spectral region, with two focal plane instruments (FPIs): the InfraRed Camera (IRC: Onaka et al., 2007) and the Far-Infrared Surveyor (FIS: Kawada et al., 2007). In this paper we focus on the results of a new processing designed to recover the diffuse galactic emission using the Far-Infrared Surveyor instrument data (FIS, Kawada et al., 2007). This ‘Diffuse All Sky Survey’ uses four wide-

band photometric filters extending across the 50 – 200 μm range (centred at 65 μm [N60, covering the range 50–80 μm], 90 μm [WIDE-S, covering 60–110 μm], 140 μm [WIDE-L, covering 110–180 μm] and 160 μm [N160, covering 140–180 μm]). These data form part of the Legacy from which we hope to fly the future SPICA far-IR mission during the next decade (Swinyard et al., 2009), and the basis for ancillary studies with other telescopes (Wada et al., 2008; White et al., 2010, 2012).

The data reduction methodology for the AKARI Diffuse All Sky Survey maps will be fully presented by Doi et al. (2012, in preparation). The detector signals were read out by Capacitive Trans-Impedance Amplifiers sampled at rates of 25.28 Hz (N60, WIDE-S) and 16.86 Hz (WIDE-L, N160), and need to be corrected for the linearity of the CTIA amplifiers and sensitivity drifts of the detectors. The integrated electrical charge was detected as a ramp, which is reset periodically at intervals of 2 seconds, 1 seconds, or every sampling depending upon the sky brightness. A correlated double sampling mode (CDS) was used for very bright regions which would otherwise have saturated the detectors. The FIS was equipped with a cold shutter to achieve absolute sensitivity calibration, providing a periodic calibration flash at intervals of about 1 minute to calibrate sensitivity drifts whose time variations were shorter than about 150 minutes. The detected signal was also corrected for glitches resulting from high-energy particle impacts, and changes to the responsivity induced by the gradual build up of these hits, which excite charged particles in the detector material. The glitches were removed from the data-stream using standard de-glitching techniques, whilst the responsivity changes were mitigated by applying an electrical voltage (on the order of 1 V) for 30 seconds to each detector pixel to flush out the charged particles (bias-boosting). The survey data were also influenced from scattered light from bright objects, especially from the moon, with an elongation angle $<30^\circ$. However, the scattered light from bright planets (Jupiter and Saturn) also need to be considered, and affected data were blanked. Additional gain and offset adjustments were made for each set of time-series data to provide first order flat-fielding.

3. LOOPS AND FILAMENTARY STRUCTURES

Loops and shells of diffuse Galactic radio emission have been known since the 1960s from radio continuum data,

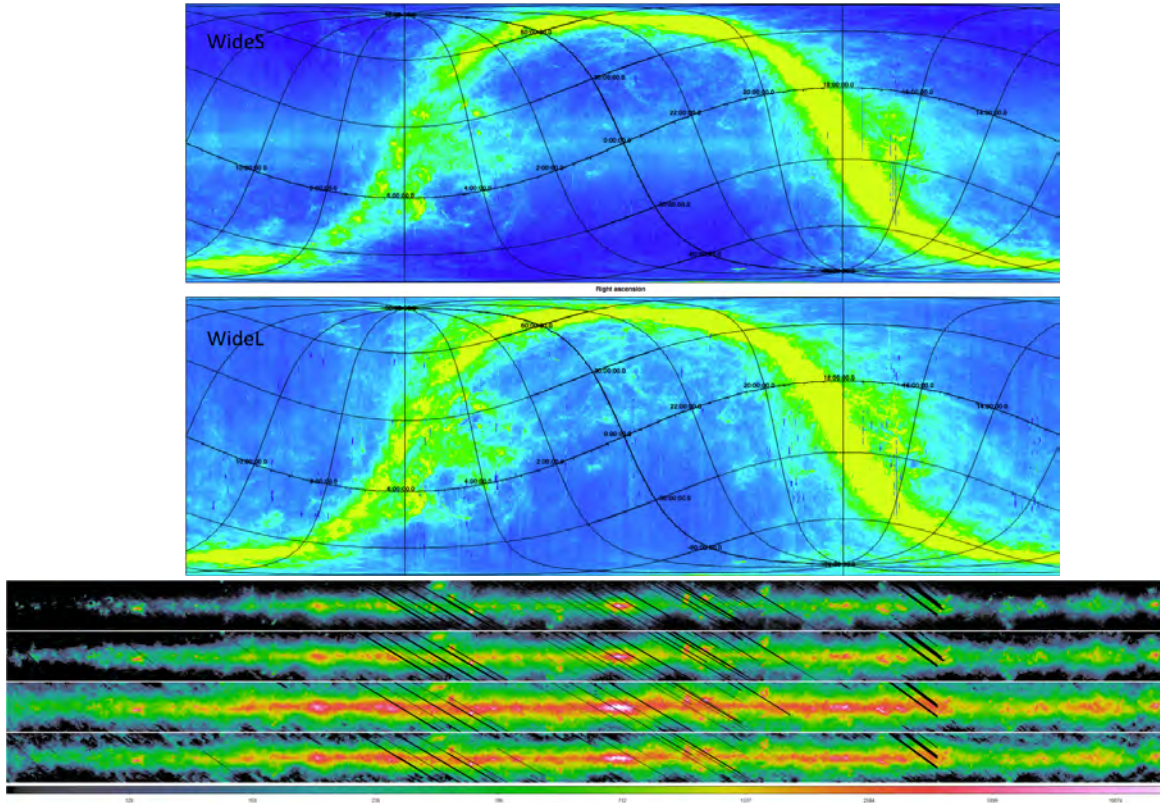


Fig. 2. [Upper two Figures] AKARI Diffuse All Sky images in the WIDE-S and WIDE-L filters. The Galactic Plane is seen as the S-like feature crossing the map that has been saturated to display the low level high Galactic latitude filamentary emission. The horizontal features seen crossing the Wide-S image show the zodiacal bands in the Solar System. The FWHM of the N60, WIDE-S, WIDE-L and N160 bands are $\sim 32.0''$, $30.2''$, $40.9''$ and $38.2''$ respectively. [Lower Figure] Galactic Plane maps in the N60, WIDE-S, WIDE-L and N160 filters.

and were followed a decade later by the detection of large atomic hydrogen, HI shells. In the 1980's the IRAS mission was able to show similar features in the far-infrared dust emission. Today the AKARI diffuse all-sky survey is providing us with the next generation to the IRAS observations of the large scale structure, whilst the ESA's Herschel Mission is revealing the complexity of these structures for a small number of specific regions. The various surveys are summarised in Figure 1, and the diffuse Galactic emission in Figure 2 [upper], whilst in Figure 2 [lower] we show the same data, but in Galactic coordinates for each of the FIS wavebands. The Galactic Centre is in the middle of these latter images.

Understanding the physical mechanisms involved in the formation of stars remains a major unsolved problem for contemporary astrophysical research, which requires understanding how the diffuse interstellar

medium (ISM) fragments and evolves to provide the initial conditions for the formation of molecular clouds. The physics is complex, but almost certainly involves compressible and magnetic turbulent motions in a thermally unstable flow. Even though turbulence organises the flow up to scales of tens of parsec (Elmegreen & Scalo, 2004), important non-linear physical processes take place at the sub-parsec scales, and well suited to AKARI's spatial resolution.

Analysis of the filamentary features in the ISM Web can be made by comparing the AKARI observations of a wide range of high and low-mass star formation regions with recent numerical simulations of supersonic (magneto)hydrodynamic turbulence. These will provide a new understanding of these filaments as the natural consequences of large-scale supersonic flows that generate complex systems of shocks, and which subsequently fragment into high-density sheets and fila-

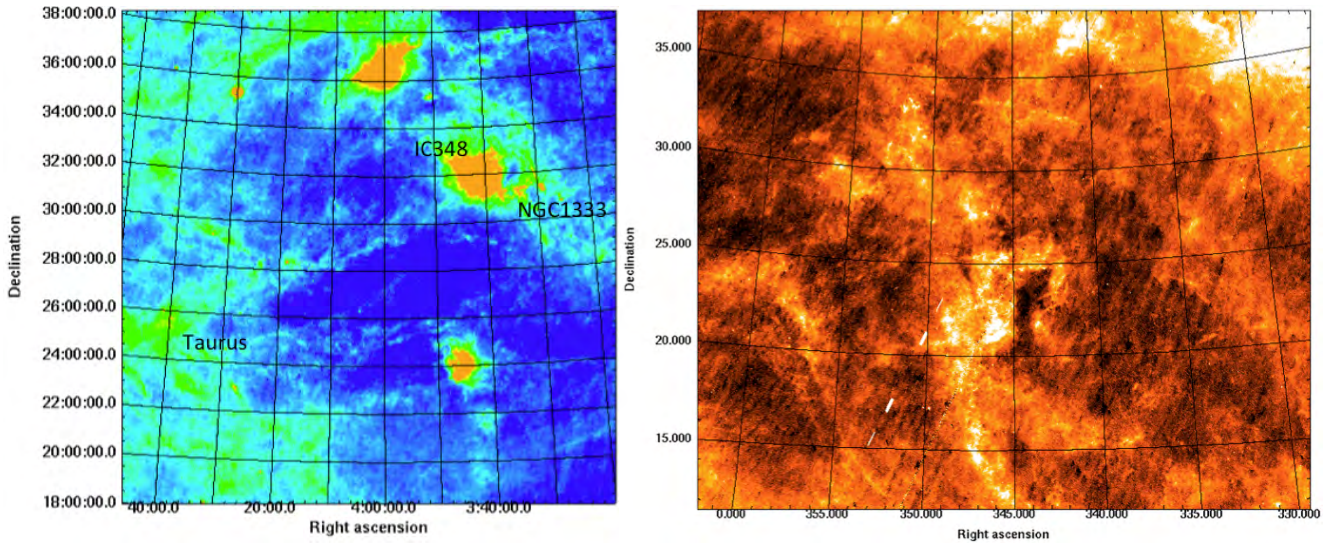


Fig. 3. AKARI All Sky Diffuse images: [left] the WIDE-S image of the Taurus and Perseus star formation regions which form part of the Gould Belt of nearby star forming regions (Ward-Thompson et al., 2007): [right] a large scale WIDE-S image of the diffuse high Galactic latitude cirrus far from the Galactic Plane.

ments. These filaments, typically having widths ~ 0.1 pc, correspond to dense, post-shock stagnation gas associated with regions of supersonic converging flows, where the kinetic energy of the turbulent motions is efficiently dissipated, and whose stability against gravitational collapse is determined by the mass per unit length. Key questions we seek to understand include:

- Are cirrus filaments shaped by magnetic effects or other processes?
- Do they trace MHD effects in the self-gravitating ISM?
- Do protostars, or cold cores, preferentially form on the filaments
- Are they the primordial structures required for star formation to occur?

3.1. Individual Regions: Taurus-Perseus and Orion

In Figures 3 and 4 we show the preliminary AKARI Diffuse maps of the Taurus and Perseus regions; a section of the diffuse high Galactic latitude emission; and finally a map of the Orion region.

Taurus is a well-studied region of low mass star formation (see Kenyon, Gomez & Whitney (2009) and Davis et al. (2010) for detailed reviews), covering an

area in excess of 100 deg^2 , which require large area maps, such as those of the AKARI Diffuse All Sky map to facilitate comparison. Kenyon & Hartmann (1995) have presented a list of ~ 300 Young Stellar Objects (YSOs) in Taurus, derived from multi-wavelength observations and complemented recently with data from the Spitzer Space Telescope (Hartmann et al., 2005; Luhman et al., 2006). Many of the youngest sources were also detected in the 1.3 mm continuum survey obtained by Motte & André (2001). The Perseus region is an intermediate star-forming environment consisting of a series of dark clouds with a mass of $\sim 1.7 \times 10^4 M_{\odot}$, extending over about 1.5×5 degrees on the sky, and adjacent to the Taurus complex. It is associated with Per OB2, the second closest OB association to the Sun, with an age < 15 My, and appears to have blown an ~ 20 deg diameter shell of atomic hydrogen into the interstellar medium, with the Perseus molecular cloud embedded in its western rim (Curtis et al., 2010).

In Figure 5 we show a comparison between an AKARI Wide-S/WIDE-L/N160 three colour image, and a recent Herschel $250 \mu\text{m}$ image of the Polaris Flare, which is a high Galactic latitude cirrus cloud, located at a distance < 150 pc. It has significant CO emission, a total gas mass of $\sim 5,500 M_{\odot}$, and somewhat colder dust grains than typical diffuse clouds. As the Polaris flare does not show any sign of star-formation activity, it is the archetype of the initial

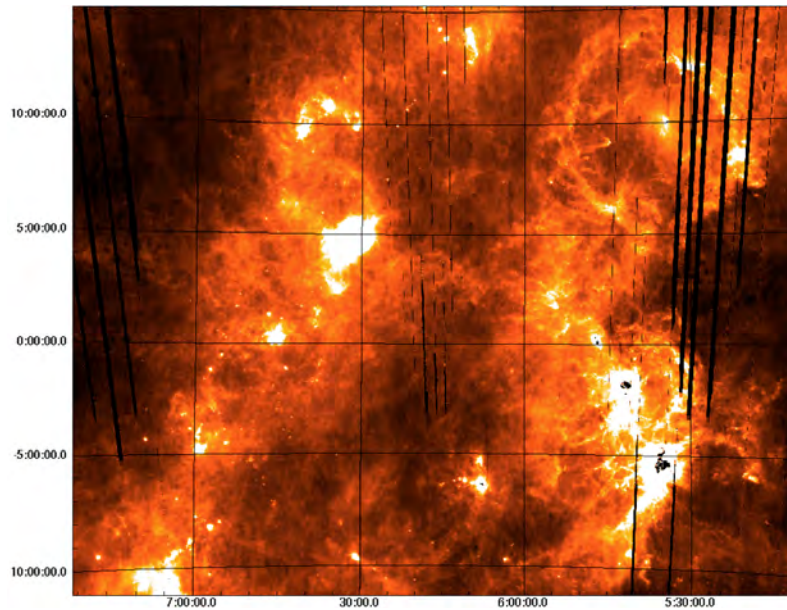


Fig. 4. Large scale AKARI All Sky Diffuse WIDE-L image of the Orion region. The dark stripes are moon avoidance regions where data are blanked to mitigate scattered moonlight. These will be eliminated in subsequent processing of the All Sky products.

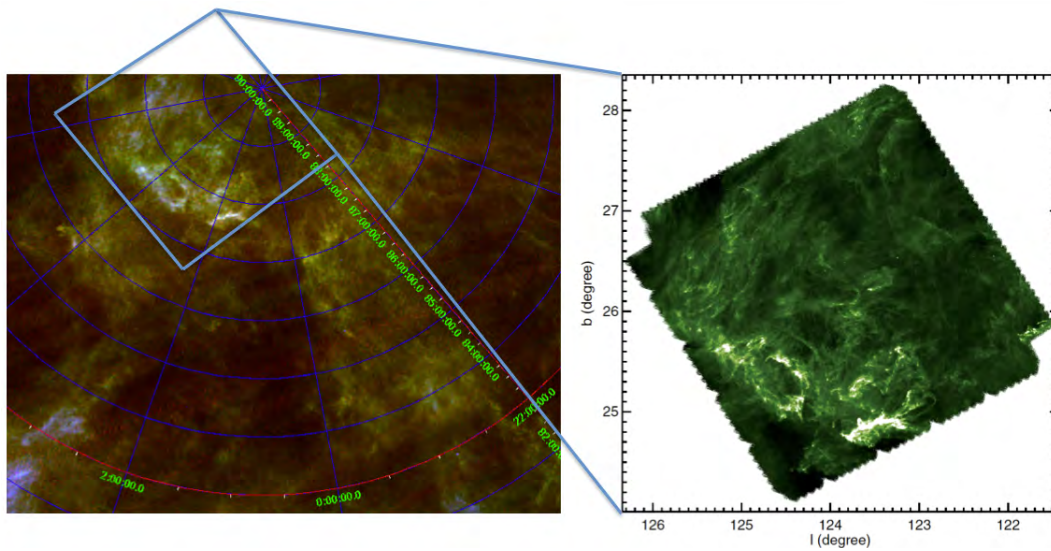


Fig. 5. [Left] AKARI Wide-S/WIDE-L/N160 three colour image of the Polaris Flare; [Right] a recent Herschel 250 μm image from Miville-Deschênes et al.(2010), showing that the AKARI data recovers most of the large scale structures seen by Herschel, whilst additionally providing coverage of much larger areas.

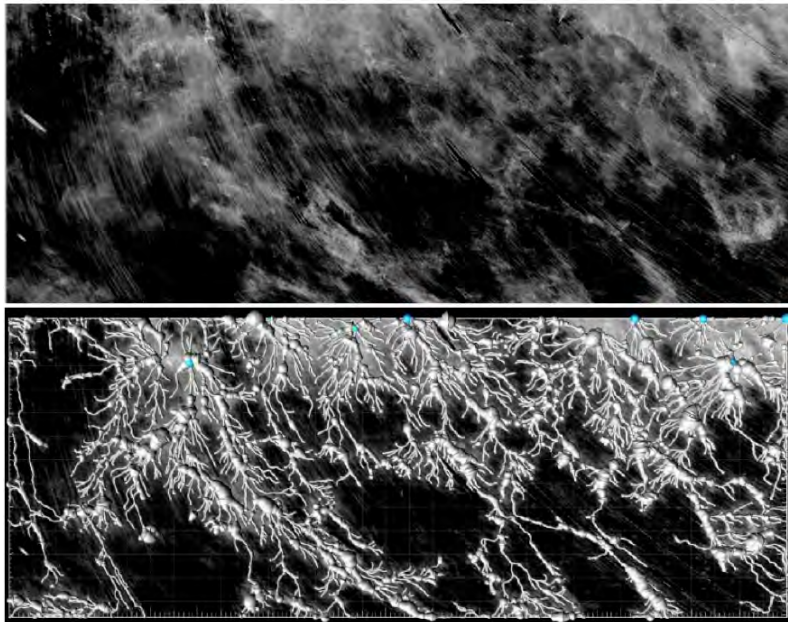


Fig. 6. [Upper]: A 30×90 degree WIDE-S images of the high Galactic latitude sky. The Andromeda Galaxy, M31, is the bright edge-on elliptical structure just above centre close to the left hand edge of the top figure. [Lower] A filament extraction using the IMARIS software package (with thanks to Dr. Delisa Garcia of www.bitplane.com).

phases of molecular cloud formation (Miville-Deschênes et al., 2010).

To analyse the filamentary structure in the ISM it is necessary to find robust ways to identify filamentary structures in the image planes: e.g. using minimum spanning tree algorithms, gradient techniques, or specific computational algorithms designed to detect filamentary or cylindrical objects. We show one example of such a deconvolution using an evaluation version of the commercial software package, IMARIS in Figure 6. Other filament extraction routines are currently being compared.

4. CONCLUSIONS

The new Diffuse All sky maps show the large scale influence of turbulence on star-formation, revealing a scenario according to which core formation occurs in two main steps: First, large-scale MHD turbulence generates a complex network of filaments in the ISM; second, the densest filaments fragment into pre-stellar cores through gravitational instability. This picture undoubtedly is matched by similar Filamentary Webs that thread and shape the properties of other galaxies.

REFERENCES

- Curtis, E. I., Richer, J. S., & Buckle, J., 2010, A Submillimetre Survey of the Kinematics of the Perseus Molecular Cloud - I. Data, *MNRAS*, 401, 455
- Davis, C. J., Chrysostomou, A., Hatchell, J., & Wouterloot, J. G. A., 2010, The JCMT Legacy Survey of the Gould Belt: a First Look at Taurus with HARP, *MNRAS*, 405, 759
- Elmegreen, B. G. & Scalo, J., 2004, *Interstellar Turbulence I: Observations and Processes*, *ARAA*, 42, 211
- Hartmann, L., Megeath, S. T., Allen, L., Luhman, K., et al., 2005, IRAC Observations of Taurus Pre-Main-Sequence Stars, *ApJ*, 629, 881
- Kawada, M., Baba, H., Barthel, P. D., et al., 2007, The Far-Infrared Surveyor (FIS) for AKARI, *PASJ*, 59, S389
- Kenyon, S. J. & Hartmann, L., 1995, Pre-Main-Sequence Evolution in the Taurus-Auriga Molecular Cloud, *ApJS*, 101, 117
- Kenyon, S. J., Gomez, M., & Whitney, B. A., 2009, in *Handbook of Star Forming Regions Vol.1*, ed. B. Reipurth, ASP Monographs, p.405
- Luhman, K. L., Whitney, B. A., Meade, M. R., Babler, B. L., et al., 2006, A Survey for New

- Members of Taurus with the Spitzer Space Telescope, *ApJ*, 647, 1180
- Miville-Deschênes, M. -A., Martin, P. G., Abergel, A., & Bernard, J. -P., 2010, Herschel-SPIRE Observations of the Polaris Flare: Structure of the Diffuse Interstellar Medium at the Sub-Parsec Scale, *A&A*, 518, L104
- Motte, F. & André, P., 2001, The Circumstellar Environment of Low-Mass Protostars: A Millimeter Continuum Mapping Survey, *A&A*, 365, 440
- Murakami, H., Baba, H., & Barthel, P. D., et al., 2007, The Infrared Astronomical Mission AKARI, *PASJ*, 59, S369
- Onaka, T., Matsuhara, H., & Wada, T., et al., 2007, The Infrared Camera (IRC) for AKARI – Design and Imaging Performance, *PASJ*, 59, 401
- Swinyard, B., Nakagawa, T., Merken, P., & Royer, P., et al., 2009, The Space Infrared Telescope for Cosmology and Astrophysics: SPICA a Joint Mission between JAXA and ESA, *Experimental Astronomy*, 23, 193
- Wada, T., Matsuhara, H., Oyabu, S., & Takagi, T., 2008, AKARI/IRC Deep Survey in the North Ecliptic Pole Region, *PASJ*, 60, S517
- Ward-Thompson, D., Di Francesco, J., Hatchell, J., Hogerheijde, M. R., et al., 2007, The James Clerk Maxwell Telescope Legacy Survey of Nearby Star-Forming Regions in the Gould Belt, *PASP*, 119, 855
- White, G. J., Pearson, C., Braun, R., & Serjeant, S., et al., 2010, A Deep Survey of The AKARI North Ecliptic Pole Field. I. WSRT 20 cm Radio Survey Description, Observations and Data Reduction, *A&A*, 517, A54
- White, G. J., Hatsukade, B., Pearson, C., Takagi, T., et al., 2012, A Deep ATCA 20 cm Radio Survey of the AKARI Deep Field South near the South Ecliptic Pole, *astro-ph 1207.2262*